IEEE Access
Multidisciplinary | Rapid Review | Open Access Journal

Received 17 February 2023, accepted 10 April 2023, date of publication 17 April 2023, date of current version 5 May 2023.

Digital Object Identifier 10.1109/ACCESS.2023.3267508

RESEARCH ARTICLE

Fully Decoupled Current Control and Current Balancing of the Modular Structure for LED Color-Mixing System

RUIHONG ZHANG[1], (Member, IEEE), ZHENG CAO[1], LINGLING CAO[1], (Member, IEEE), AND E. PENG[2], (Member, IEEE)

[1]Harbin Institute of Technology, Shenzhen 518055, China
[2]Harbin Institute of Technology, Harbin 150001, China

Corresponding author: E. Peng (epeng@hit.edu.cn)

This work was supported in part by the Stable Support Plan for Shenzhen Universities under Project GXWD20201230155427003-20200823171314001 and Project 20200823111955001.

ABSTRACT For LED color-mixing, the different color LEDs need to be controlled independently, so a fully decoupled current control and current balancing of the modular structure is proposed for LED color-mixing system. The capacitive current-balancing structure is combined with the quasi-boost converter to realize the decoupled current control and current balancing in each module. The capacitive current-balancing structure is based on the relative reactance of the capacitor with respect to the equivalent resistance of the associated LED string. The inductor in quasi-boost converter is used to further stable the output current flowing through each LED string, and the switch in quasi-boost converter for controlling the current of each LED string adopts the parallel connection to protect LEDs from the current-spike caused by the switch. The structure is modularity and scalability so that the different color LEDs can be added and removed easily. Compared with SIMO (Single-Inductor-Multiple-Output) structure, the proposed structure has no cross-coupling issues. The LED string currents working with PWM mode have a good current-balancing performance since the equivalent resistance of LED string is much smaller than the reactance of capacitors. In addition, the resonant capacitors separate the grounds of the power source and LED strings, so all the switches in parallel with LED strings do not need the isolated gate drivers. A prototype with RGB modules has been built and evaluated, and the experimental results have a good agreement with the theoretical analysis.

INDEX TERMS Decoupled current control, current balancing, lighting technology, color-mixing.

NOMENCLATURE

d_k : The duty ratio of k-th LED string.
d_{S_k} : The duty cycle of the switch S_k.
v_{LS_k} : The voltage of k-th LED string.
V_{LS_k} : The voltage amplitude of k-th LED string.
i_{LS_k} : The current of k-th LED string.
I_{LS_k} : The current amplitude of k-th LED string.
v_{L_k} : The voltage across the inductor L_k.
v_{S_k} : The voltage across the switch S_k.
R_{LS_k} : The equivalent resistance of k-th LED string.
f_k : The switching frequency of the switch S_k.
f_Q : The switching frequency of the switches Q_1 and Q_2.
ω_Q : The angular switching frequency of the switches Q_1 and Q_2.
d_Q : The switching duty cycle of the switch Q_1.
P_k : The output power of k-th LED string.

The associate editor coordinating the review of this manuscript and approving it for publication was Jiajie Fan.

I. INTRODUCTION

The research of Psychology presents that colors can create certain mood, influence the decisions people make and even affect the appetites of some people [1]. Study on visible light communication suggests that RGB-mixed white light can provide higher rate of communication than

phosphor-converted white LEDs [2]. Meanwhile, RGB-mixed white light will have higher color rendering index (CRI) than phosphor-converter LED light. More channels, such as RGBA (Red-Green-Blue-Amber), RGBAW (Red-Green-Blue-Amber-White), RGBAOCP (Red-Green-Blue-Amber-Orange-Cyan-Purple) etc. for color mixing are constantly emerging [3]. Therefore, the research on the multi-channel color-mixing systems draws more and more attention in recent years.

The studies indicate that it is essential for LED color-mixing to use the independent current-controlled structure. A straightforward structure with independent current control capability is based on using a dedicated converter, such as buck, boost and buck-boost, for each LED string. The input of these converters shares the same DC bus [4], [5], [6]. This structure has high efficiency and is easy for modular design. However, it suffers from huge number of components and high cost. In order to decrease the number of components, the current regulator working under PWM mode is proposed in [7], [8], and [9]. Adding a switch for each output and regulating the duty cycle of this switch can achieve independent current adjustment. The current ratio of LED strings with different color is regulated by PWM signal. However, the power loss in this structure is greatly dependent on the forward voltage of LED string and becomes more severe when the forward voltage is low, so it suffers from high power loss. In order to decrease form factor while maintaining or improving power efficiency, a Single-Inductor-Multiple-Output (SIMO) structure was proposed in [10], [11], [12], [13], [14], [15], [16], [17], [18], and [19]. However, the achievable number or maximum current of LED strings is practically limited with this structure. The structure based on buck, boost or buck-boost converter, in which LED strings are series with switches, was proposed in [10], [11], [12], [13], [14], and [15]. The most distinctive advantage of this structure is that the switches have common source. Thus, non-isolated gate-driver is needed. However, the switching noise will decrease the life-span of LEDs. In order to solve this problem, reference [18] puts the switches in parallel with LED strings. However, many isolated driving circuits are required. In addition, whether the switches are in series or in parallel with LED strings, the common characteristic of SIMO LED drivers is that there is only one switch operating in ON-state at any time with the time-multiplexing fashion. Therefore, sophisticated switching sequence is required. In particular, it is necessary to consider the effect of cross-coupling. In order to address this issue, reference [19] proposed a fully Switched-Capacitor-Controlled LCC (SCC-LCC) resonant network for the independent control using two switches for each LED string, so it also suffers from huge number of components and high cost.

In color-mixing system, the cross-coupling among the different color channels and the isolated drivers for all the switches will increase the control complexity. Meanwhile, since compared with the same color LEDs, the currents of the multi-color LEDs will be much more unbalanced as the voltages and thermal sensitivities of different color LEDs have a big difference, the current-unbalancing is another issue for LED color-mixing. In addition, PWM dimming is prefer for color-mixing as the current amplitude will cause the color shift. However, it is easy for PWM dimming to cause the current spike which will shorten the lifespan of LEDs. At last, it is better to have the galvanic isolation between the LED modules and the power module to enhance the safety of product. So far, it is difficult to build such a structure to solve all the above-mentioned issues in the prior-art technologies. Based on this, a new structure capable of independent current control and current balancing for multicolor LED strings based on [20] and [21] is proposed to solve most above-mentioned problems at once. Compared with [20] and [21], the proposed structure has the following characteristics: (1) having the capability of independent current control; 2) capable of PWM and amplitude dimming; 3) without requiring the energy-recycling circuit. The proposed structure is based on using a half-bridge resonant driver to drive multiple dimming modules. The input current of each dimming module is balanced by a capacitive current-balancing circuit. The capacitive current-balancing circuit is combined with the quasi-boost converter to realize the fully decoupled current control and current balancing in each module. The inductor in quasi-boost converter is used to further stable the output current flowing through each LED string, and the switch in quasi-boost converter for controlling the current of each LED string adopts the parallel connection to protect LEDs from the current-spike caused by the switch. The system works in the inductive-region to realize the soft-switching. In the proposed structure, any LED string can be totally turned on or off when the system is running. Table 1 shows the comparison of the various independent current-controlled structures for LED color-mixing. It is found that the proposed structure is ideally suited for color mixing. Moreover, the control complexity of the proposed structure is greatly reduced because of no cross-coupling issues, non-isolated drivers and self-balancing current function. Thus, although the number of components is not reduced, the overall cost of the proposed structure will be not too high.

In summary, the proposed structure has the following advantages:

1) No cross-coupling issues — different modules are fully decoupled with each other without cross-interference and cross-regulation problems;
2) No current spike — life-span of LEDs is not affected because the switch is in parallel with each LED string;
3) Current-balancing function — currents of LED strings with different color can be balanced automatically;
4) Non-isolated gate-driver circuits — All the switches share the same ground;
5) Modularity — module can be added and removed easily;
6) High stability — the structure can be working normally even if all the LEDs fail;

TABLE 1. Comparison of the various independent current-controlled structures for LED color-mixing.

Structures	References	Number of Components				Galvanic isolation	Non-isolated Gate drivers	No Current Spike	No Cross-Coupling	Current-balancing	PWM Dimming
		Inductors	Capacitors	Diodes	MOSFETs						
Dedicated converters	[4]-[5]	N	N	N	N	×	×	√	√	×	×
	[6]	N	N	0	$2N$	×	×	√	√	×	×
Current regulator	[7]-[8]	0	0	0	$2N$	×	√	×	×	√	√
SIMO structure	[10]	0	N	N	N-1	×	√	√	×	×	×
	[12]-[13]	0	0	0	N	×	√	×	×	×	×
	[14]-[16]	0	N	N	N	×	√	√	×	×	×
	[17]	0	N	0	$2N$	×	√	×	×	×	×
	[18]	0	0	N	N	×	×	√	×	√	√
Resonant structure	[19]	0	$3N$	$4N$	$2N$	×	×	√	√	√	×
Proposed structure		N	$3N$	$3N$	N	√	√	√	√	√	√

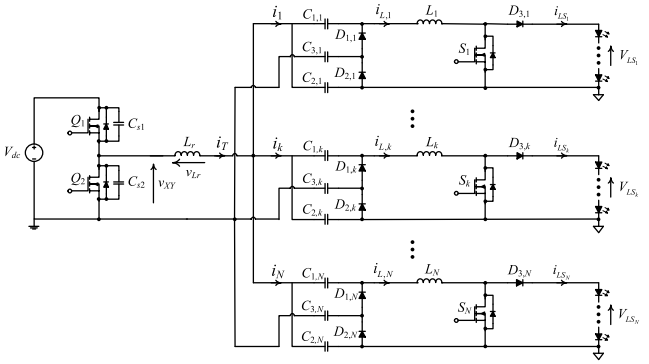

FIGURE 1. Generalized structure of the proposed LED driver.

7) High safety — The input and output are all isolated by capacitors.

The paper is organized as follows. In Section II, the operating principle is illustrated, including the derivation of the equivalent circuit of module, the analyses of whole system and the illustrative example of RGB strings. The experimental results are presented in Section III, and the conclusions follow in the last section.

II. OPERATION PRINCIPLE

Figure 1 shows the generalized structure of the proposed LED driver having N modules. Each module consists of capacitors $C_{1,k}$, $C_{2,k}$ and $C_{3,k}$, diodes $D_{1,k}$, $D_{2,k}$ and $D_{3,k}$, inductor L_k and switch S_k. The grounds of the power source and LED strings are separated by the capacitors $C_{1,k}$, $C_{2,k}$ and $C_{3,k}$. The values of $C_{1,k}$ and $C_{2,k}$ are the same. The diodes $D_{1,k}$ and $D_{2,k}$ are used to rectify the currents, and $D_{3,k}$ is used to limit the reverse current upon turning on the switch S_k. The switch S_k is used to control the LED string current. The inductor L_k is used to provide current source for the LED string and decrease the current ripple flowing through the strings. Though there is one inductor in each module, its value is very small. The inductor L_k, switch S_k and diode $D_{3,k}$ can be seen as a quasi-boost converter. All modules have their inputs connected to the output of half-bridge switching network, formed by switches Q_1 and Q_2, through inductor L_r. The capacitors $C_{1,k}$ and $C_{2,k}$ serve as part of the resonant components. As $C_{1,k}$ and $C_{2,k}$ are small, their reactance are designed to be much larger than the equivalent resistance of the LED strings for current balancing.

A. EQUIVALENT CIRCUIT OF K-TH MODULE

Figure 2 shows the steps of deriving the equivalent circuit. The circuit of k-th module has been shown in Figure 2(a). As the function of capacitor $C_{3,k}$ is used to block DC current, and the diode $D_{3,k}$ is only used to limit the reverse current upon turning on the switch S_k, they are all neglected in this analysis as shown in Figure 2(b). The switch S_k, inductor L_k and k -th LED string can be equivalent to a resistor $R_{L,k}$ as shown in Figure 2(c). The waveforms of v_{S_k} and $i_{L,k}$ are shown in Figure 3. The voltage of v_{S_k} is square wave, and its amplitude is LED string voltage, V_{LS_k}. The current $i_{L,k}$ is fairly constant, and equal to the amplitude of LED string current, I_{LS_k}.

The switch S_k is used to control the LED string current, and the average value of voltage across the switch S_k, v_{S_k} is:

$$\bar{v}_{S_k} = \left(1 - d_{s_k}\right) V_{LS_k} = d_k \; V_{LS_k} \tag{1}$$

where d_{s_k} is the duty cycle of the switch S_k, and d_k and V_{LS_k} are the duty ratio and the voltage amplitude of k-th LED string respectively.

By using KVL in Figure 2(b),

$$\bar{v}_{L,k} = \bar{v}_{S_k} - \bar{v}_{L_k} \tag{2}$$

where $\bar{v}_{L,k}$, $\bar{v}_{S_k}$, $\bar{v}_{L_k}$ are the average values of voltage $v_{L,k}$, v_{S_k}, v_{L_k}.

As the average voltage across an inductor is zero,

$$\bar{v}_{L_k} = 0 \tag{3}$$

By putting (3) into (2),

$$\bar{v}_{L,k} = \bar{v}_{S_k} \tag{4}$$

The equivalent resistor in Figures 2(b) and (c), $R_{L,k}$ is

$$R_{L,k} = \frac{\bar{v}_{L,k}}{\bar{i}_{L,k}} \tag{5}$$

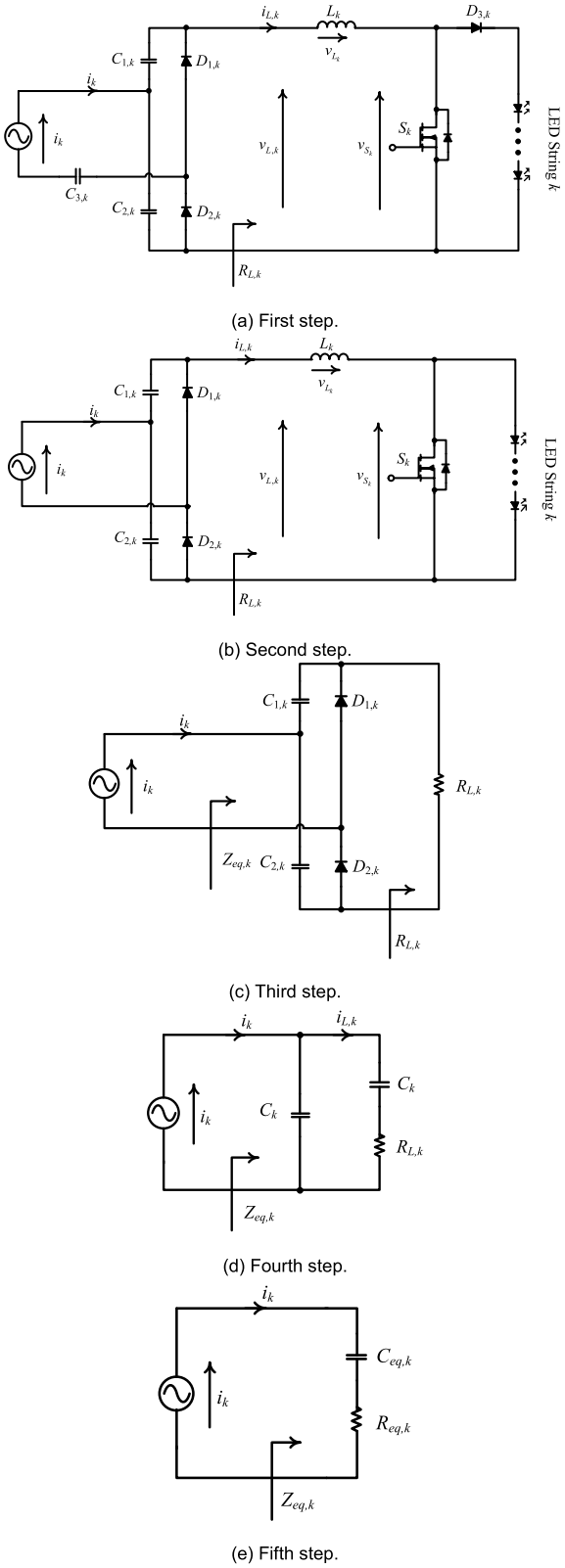

FIGURE 2. Equivalent circuit of module k.

The average value of current $i_{L,k}$, $\bar{i}_{L,k}$ is equal to the current amplitude of k-th LED string, I_{LS_k}, that is

$$\bar{i}_{L,k} = I_{LS_k} \tag{6}$$

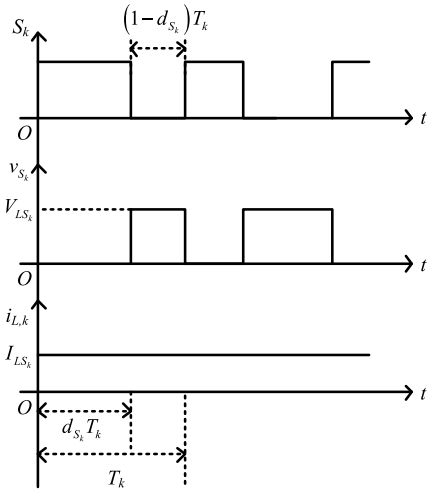

FIGURE 3. Waveform of v_{Sk} and $i_{L,k}$.

By putting (1), (4), (6) into (5),

$$R_{L,k} = \frac{d_k\ V_{LS_k}}{I_{LS_k}} = d_k\ R_{LS_k} \tag{7}$$

where R_{LS_k} is the equivalent resistance of k-th LED string. The current i_k, sinusoidal waveforms, in positive or negative half-cycle all flows two parallel branches as shown in Figure 2(c). One branch consists of a capacitor, and another one consists of one capacitor and the equivalent resistance of LED string in series as shown in Figure 2(d). Assume that capacitors $C_{1,k}$ and $C_{2,k}$ are the same.

$$C_{1,k} = C_{2,k} = C_k \tag{8}$$

Thus, $R_{L,k}$ is referred to the ac side of the diode half-bridge circuit in Figure 2(d).

The equivalent impedance formed by C_k and $R_{L,k}$ is $Z_{eq,k}$,

$$\begin{aligned} Z_{eq,k} &= R_{eq,k} + \frac{1}{j\ \omega_Q\ C_{eq,k}} \\ &= \frac{1}{\omega_Q^2\ R_{L,k}^2\ C_k^2\ +\ 4}\ R_{L,k} + \frac{1}{j\ \omega_Q\ \frac{\omega_Q^2\ R_{L,k}^2\ C_k^2 + 4}{\omega_Q^2\ R_{L,k}^2\ C_k^2 + 2}\ C_k} \end{aligned} \tag{9}$$

where $\omega_Q\ =\ 2\ \pi\ f_Q$.

According to (9), $R_{eq,k}$ and $C_{eq,k}$ as shown in Figure 2(e) are

$$R_{eq,k} = \frac{1}{\omega_Q^2\ R_{L,k}^2\ C_k^2\ +\ 4}\ R_{L,k} \tag{10}$$

$$C_{eq,k} = \frac{\omega_Q^2\ R_{L,k}^2\ C_k^2\ +\ 4}{\omega_Q^2\ R_{L,k}^2\ C_k^2\ +\ 2}\ C_k \tag{11}$$

The equivalent resistance of k-th LED string, R_{LS_k} is designed much smaller than the reactance of the capacitors $C_{1,k}$ and $C_{2,k}$ for current-balancing, by using (7) and (8),

$$R_{L,k} \ll \frac{1}{\omega_Q\ C_k} \tag{12}$$

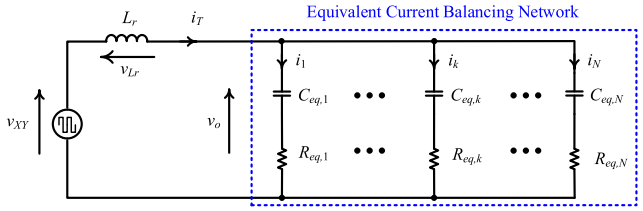

FIGURE 4. Equivalent circuit of whole system.

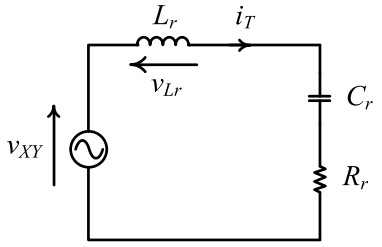

FIGURE 5. Equivalent resonant of whole system for mathematic analysis.

By putting (12) into (10) and (11), $R_{eq,k}$ and $C_{eq,k}$ can be further simplified into

$$R_{eq,k} = \frac{R_{L,k}}{4} \tag{13}$$

$$C_{eq,k} = 2\ C_k \tag{14}$$

B. STRUCTURAL ANALYSIS

Figure 2(e) shows the final equivalent circuit for k-th module, and the equivalent circuit of whole system is shown in Figure 4. The voltage source v_{XY} is a high-frequency square-wave voltage produced by a half-bridge switching network. The equivalent current-balancing network is composed of capacitors and resistors. As the reactance of capacitor is much larger than the equivalent resistance of LED string, it is possible to balance the currents $i_1, \ldots, i_k, \ldots, i_N$ by ensuring that a considerably larger proportion of v_o appears across the equivalent current-balancing capacitors $C_{eq,k}$, hence the LED string current is mainly determined by the capacitive impedance, and is less sensitive to the variation of LED strings.

In Figure 4, the total current i_T can be expressed as

$$i_T = \sum_{k=1}^{N} i_k \tag{15}$$

Because of the current-balancing network, currents i_1, $i_2, \ldots, i_k$ are approximately equal.

$$i_1 \doteq i_2 \cdots \doteq i_k \cdots \doteq i_{N-1} \doteq i_N \tag{16}$$

In Figure 2(d), since the equivalent resistor $R_{L,k}$ is much smaller than the impedance of capacitors C_k, the current i_k is approximately equal to two times of the current $i_{L,k}$.

$$i_{L,k} = \frac{1}{2\,\pi} \int_0^{\pi} i_k\ d\ \omega_s t = \frac{1}{\pi} |i_k| \tag{17}$$

where $|i_k|$ is the amplitude of i_k.

According to Figure 2(b), the current $i_{L,k}$ is equal to the current amplitude of k-th LED string, I_{LS_k},

$$i_{L,k} = I_{LS_k} \tag{18}$$

For current-balancing network,

$$I_{LS_1} \doteq I_{LS_2} \cdots \doteq I_{LS_k} \cdots \doteq I_{LS_{N-1}} \doteq I_{LS_N} = I_{LS} \tag{19}$$

From (15)-(19),

$$|\ i_T\ | \ = \ \pi \sum_{k=1}^{N} I_{LS_k} = N\ \pi\ I_{LS} \tag{20}$$

For simplicity, the following assumptions are made,

$$R_{eq,1} \doteq R_{eq,2} \doteq \cdots \doteq R_{eq,N} \doteq R_{eq} = \frac{1}{N} \sum_{k=1}^{N} R_{eq,k} \tag{21}$$

$$C_{eq,1} \doteq C_{eq,2} \doteq \cdots \doteq C_{eq,N} \doteq C_{eq} = \frac{1}{N} \sum_{k=1}^{N} C_{eq,k} \tag{22}$$

By putting (7) and (13) into (21),

$$R_{eq} = \frac{1}{N} \sum_{k=1}^{N} R_{eq,k} = \frac{1}{4\,N} \sum_{k=1}^{N} d_k R_{LS_k} \tag{23}$$

By putting (14) into (22),

$$C_{eq} = \frac{1}{N} \sum_{k=1}^{N} C_{eq,k} = \frac{2}{N} \sum_{k=1}^{N} C_k \tag{24}$$

Figure 5 shows the equivalent resonant circuit of whole system for mathematic analysis. L_r, R_r and C_r are the equivalent inductor, resistor and capacitor, respectively.

With (21) and (22), according to the structure as shown in the Figures 4 and 5,

$$R_r = \frac{R_{eq}}{N} \tag{25}$$

$$C_r = N\ C_{eq} \tag{26}$$

By putting (23) and (24) into (25) and (26),

$$R_r = \frac{1}{4\,N^2} \sum_{k=1}^{N} d_k R_{LS_k} \tag{27}$$

$$C_r = 2 \sum_{k=1}^{N} C_k \tag{28}$$

In Figure 1, the switches Q_1 and Q_2 are operated with duty cycle 0.5, so the waveform of v_{XY} is square wave. For the sake of simplicity, the analysis only takes the fundamental

switching frequency component into account. The fundamental component of v_{XY}, v_{XY}^F is

$$v_{XY}^F(t) = V_{XY}^F \cos(\omega_Q t) = \frac{2V_{dc}}{\pi} \cos(\omega_Q t) \quad (29)$$

where $V_{XY}^F = \frac{2}{T_Q} \int_{-\frac{T_Q}{2}}^{\frac{T_Q}{2}} v_{XY}(t) \cos(\omega_Q t)\, dt = \frac{2V_{dc}}{\pi}$.

In Figure 5, by using Ohm's law,

$$|i_T| = \frac{|v_{XY}^F|}{\sqrt{R_r^2 + \left(\omega_Q L_r - \frac{1}{\omega_Q C_r}\right)^2}} \quad (30)$$

By putting (27)-(30) into (20), the current amplitude of LED string current is

$$I_{LS} = \frac{2V_{dc}}{N\pi^2 \sqrt{\left(\frac{1}{4N^2}\sum_{k=1}^{N} d_k R_{LS_k}\right)^2 + \left(\omega_Q L_r - \frac{1}{2\omega_Q \sum_{k=1}^{N} C_k}\right)^2}} \quad (31)$$

The power of k-th LED string, P_k is

$$P_k = v_{LS_k} i_{LS_k} \quad (32)$$

The total power consumed by all LED strings, P_t, is

$$P_t = \sum_{k=1}^{N} P_k = \sum_{k=1}^{N} v_{LS_k} i_{LS_k} \quad (33)$$

The switch S_k is parallel with the LED string k, so

$$v_{LS_k} = v_{S_k} \quad (34)$$

By putting (1) and (34) into (33),

$$P_t = \sum_{k=1}^{N} P_k = \sum_{k=1}^{N} d_k V_{LS_k} I_{LS_k} \quad (35)$$

C. ILLUSTRATIVE EXAMPLE OF RGB STRINGS

As we all know, RGB color mixing is the most popular solution, and the triangle surrounded by RGB color points covers most area on CIE1931 chromaticity chart. Therefore, the control for RGB color mixing is taken as an example, so three modules are analyzed, namely, $k = 1, 2, 3$. RGB color strings are connected with Modules 1, 2 and 3. For a better illustration to the analysis, Modules 1, 2 and 3 are substituted with Modules R, G and B, respectively. Thus, in the following analysis, $k = R, G, B$. d_{s_R}, d_{s_G} and d_{s_B} represent the duty cycles of switches S_R, S_G and S_B, respectively. Based on Equation (31), the relationship between LED string current amplitude and switching frequency of Q_1 and Q_2 is shown in Figure 6. As the structure can perform current-balancing function, the currents flowing through all LED strings are approximately equal as represented in Equation (19). Red,

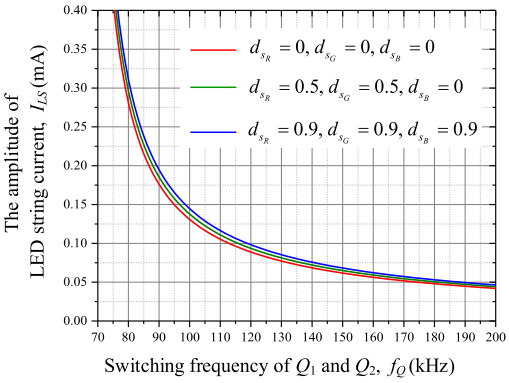

FIGURE 6. Relationship between LED string current amplitude and switching frequency of Q1 and Q2 with the different ratios of RGB LEDs.

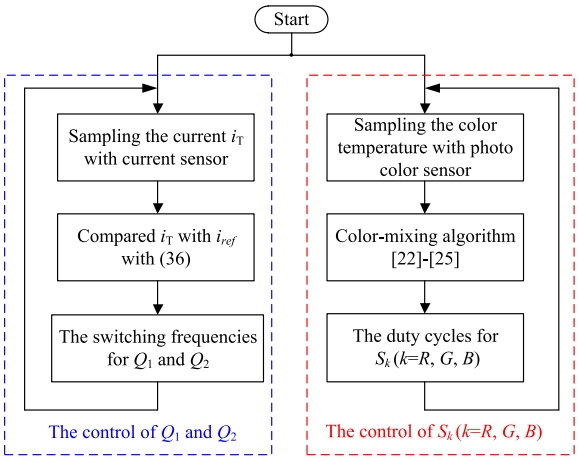

FIGURE 7. Flow chart of the control strategy for the proposed structure.

green and blue lines in Figure 6 denote the amplitude of LED string current when $d_{s_R} = 0$, $d_{s_G} = 0$, $d_{s_B} = 0$, $d_{s_R} = 0.5$, $d_{s_G} = 0.5$, $d_{s_B} = 0$ and $d_{s_R} = 0.9$, $d_{s_G} = 0.9$, $d_{s_B} = 0.9$, respectively. It can be seen that the amplitude of LED string current decreasing with the switching frequency of the switches Q_1 and Q_2 increasing is basically independent of the duty cycles of the switches S_R, S_G and S_B. Based on this, a flow chart of the control strategy for the proposed structure is shown in Figure 7. Since the controls of switches Q_1, Q_2 and S_k are independent, the control of the proposed structure can be divided into two independent loops. One is for the control of Q_1 and Q_2, and another is for the control of S_k. The two control loops are stopped until the whole system is turned off.

The first control loop is used to regulate the amplitude of LED string current for controlling the switching frequencies of Q_1 and Q_2. The input current i_T [i.e., i_T (n)] is sampled and is compared with two reference bands $i_{ref} - \Delta i_{ref}/2$ and $i_{ref} + \Delta i_{ref}/2$, where i_{ref} is the reference input current and Δi_{ref} is the width of the bands. The switching frequency f_Q in the next sampling cycle [i.e., f_Q $(n+1)$] is adjusted according

TABLE 2. Switching state for switches S_k ($k = R, G, B$).

Switching Sates No.	S_R	S_G	S_B
1	0	0	0
2	0	0	1
3	0	1	0
4	0	1	1
5	1	0	0
6	1	0	1
7	1	1	0
8	1	1	1

Note: "0" represents "OFF", and "1" represents "ON".

to the following rules:

$$f_Q(n+1) = \begin{cases} f_Q(n) - \Delta f_Q, & \text{if } i_T(n) < i_{ref} - \frac{\Delta i_{ref}}{2} \\ f_Q(n) + \Delta f_Q, & \text{if } i_T(n) > i_{ref} + \frac{\Delta i_{ref}}{2} \\ f_Q(n) & \text{Other} \end{cases} \tag{36}$$

where $f_Q(n)$ is the switching frequency in the current sample and Δf_Q is the predefined change in the switching frequency.

The second control loop is used to regulate the color temperature of the color-mixing system for controlling the switches S_k ($k = R, G, B$). The proposed structure is a general structure which suits for various color-mixing algorithm [22], [23], [24], [25]. Since switches S_R, S_G and S_B are independent of each other, they will have 8 switching states as shown in Table 2. In Table 2, "1" represents the switch in the "ON" state, and "0" represents the switch in the "OFF" state. Figure 8 shows the operating modes of RGB strings in 8 modes. As the equivalent resistance of LED string is designed to be much smaller than the reactance of capacitors, the transitions among 8 operating modes have little influence on the working of the system.

Mode 1 [000] — Switches S_R, S_G and S_B are all turned off, So the currents are all flowing through RGB LED strings.

Mode 2 [1] — Switches S_R and S_G are all turned off, and only switch S_B is in the "on" state, so the blue LED string is bypassed by switch S_B.

Mode 3 [10] — The green LED string is bypassed. The red and blue LED strings are turned on, and the green LED string is turned off.

Mode 4 [11] — Only Red LED string is turned on, so when the red color is needed, the converter will work in this mode all the time.

Mode 5 [100] — The green and blue LED strings are turned on, and the red LED string is turned off.

Mode 6 [101] — Only green LED string is turned on, so when the green color is needed, the converter will work in this mode all the time.

TABLE 3. Component values used in the prototype.

Component	Value
Q_1 and Q_2	IRFB5620PBF
L_r (L_{r1} and L_{r2})	50uH
$C_{1,k}$ and $C_{2,k}$	3.3 nF (film capacitor)
$C_{3,k}$	1 μF (film capacitor)
L_k	1mH
S_k	FDN86246

Mode 7 [110] — Only the blue LED string is turned on, so when the blue color is needed, the converter will work in this mode all the time.

Mode 8 [111] — Switches S_R, S_G and S_B are all turned on, so the currents of RGB LED strings are all 0.

According to the above analysis, the proposed structure can realize any chromaticity coordinate, including the boundary and points of RGB triangular in CIE1931 chromaticity chart. For the simplicity of the analysis, assume all the switches turn on at the same time at the starting point of one switching period. If $0 < d_R, d_G, d_B < 1$, there are 13 scenarios for switching sequences, and if $0 \leq d_R, d_G, d_B \leq 1$, there are 38 scenarios for switching sequences. The analysis of the switching sequences when $0 \leq d_R, d_G, d_B \leq 1$ is similar with the analysis when $0 < d_R, d_G, d_B < 1$, herein they are neglected.

Figure 9 shows the switching sequences of the switches S_R, S_G and S_B under the 13 scenarios when $0 < d_R, d_G, d_B < 1$. It can be seen that the operating modes are switched among 4 switching states at most in each scenario, and they can be switched over among 8 modes arbitrarily. The different modules are fully decoupled with each other without cross-interference and cross-regulation problems. The proposed fully decoupled current-controlled structure simplifies the color-mixing algorithm as it does not need to consider the switching sequences. Therefore, any color mixing algorithm can be verified based on the proposed fully decoupled current control structure.

III. EXPERIMENTAL RESULTS

A 36W prototype with RGB channels as shown in Figure 10 has been built and each LED channel is consisted of 12 LEDs. The power circuit which consists of two switches for half-bridge and the inductor L_r (L_{r1} and L_{r2}) for resonance is in the left half part of PCB board. Multi-channel modules (e.g. RGB modules) are in the right half part of PCB board. It can be seen that the grounds of power source and LEDs are separated by the film capacitors, so the grounds of LED strings are connected together and the switches for controlling RGB LED strings do not need the isolated drivers. The different color LEDs can be added or removed as needed with the power circuit remaining unchanged. In addition, the Micro-Controller Unit (MCU) and the photo color sensor are

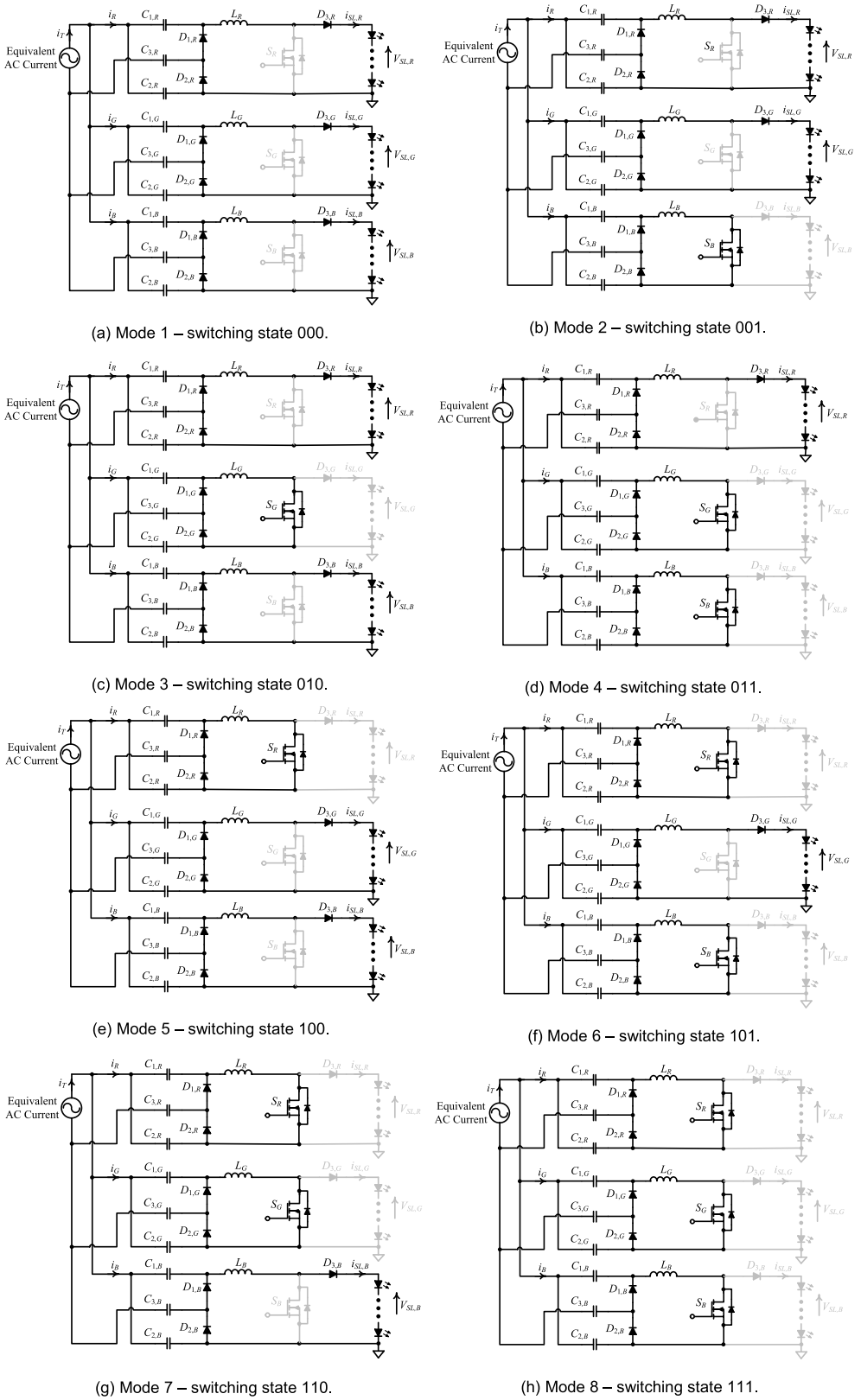

FIGURE 8. Operating modes of RGB strings.

in the upper-right portion of PCB board. The input data of MCU is from the photo color sensor and the output of MCU is PWM signal to control the duty cycles of different color LED channels. Table 3 shows the component values used in the prototype. Figure 11(a)-(d) shows the waveforms of the string voltages and currents of red and green strings or red

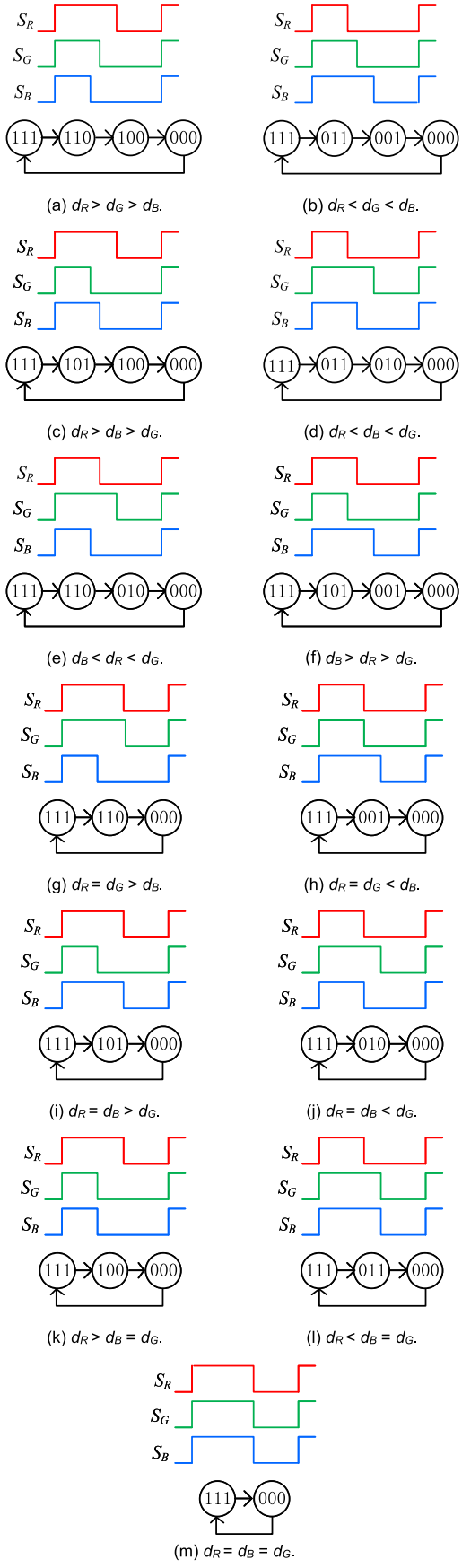

FIGURE 9. Switching sequences when $0 < d_R, d_G, d_B < 1$.

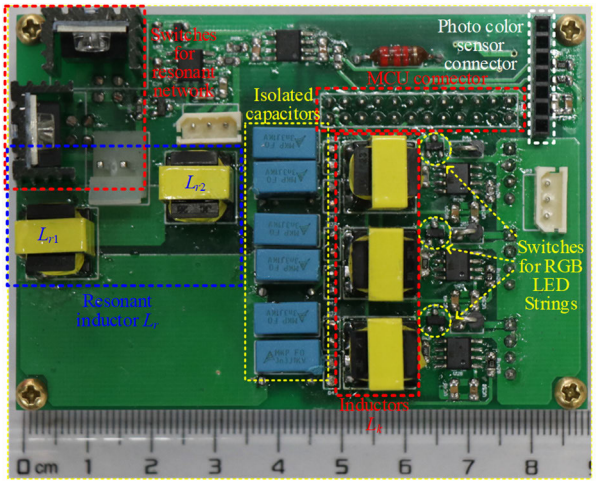

FIGURE 10. Hardware implementation.

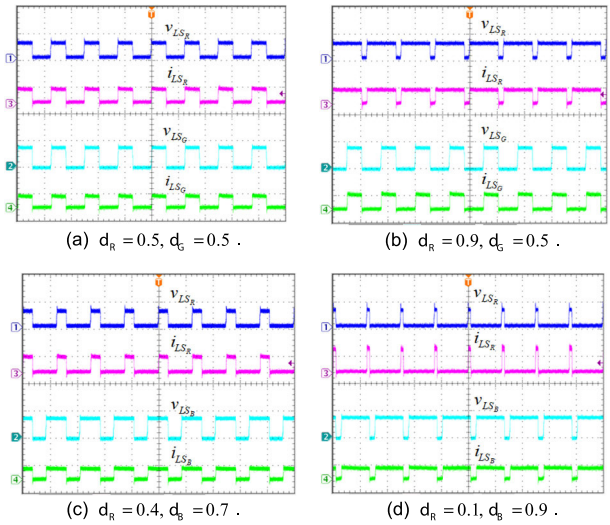

FIGURE 11. The voltage and current of the LED strings (i_{LS_R}, i_{LS_G}, i_{LS_B}: 500mA/div, v_{LS_R}, v_{LS_G}, v_{LS_B}: 50V/div, $k = R, G, B$, Timebase: 4μs/div).

and blue strings at different duty cycles. It can be seen that the amplitudes of two strings' currents are very close even if the RGB strings' voltages have great differences. Moreover, the different color LED strings can be controlled independently without the cross-coupling issues. Figure 12(a)-(d) shows the current waveforms of the input module and LED strings. It can be seen that the duty ratio of any LED string current can be varied between 0 and 1, and the input current i_k is independent from the output LED string current. The proposed structure has a good current balancing function and the current amplitude can always be maintained constant. The independence between the control of main switches and the switches for controlling the LED strings is further verified. Figure 13(a)-(d) shows the key waveforms at different duty cycles. It can be seen that the input current i_T always lags the voltage v_{XY}. Thus, the switches Q_1 and Q_2 are always soft switched. Figure 14 shows the system efficiency versus the

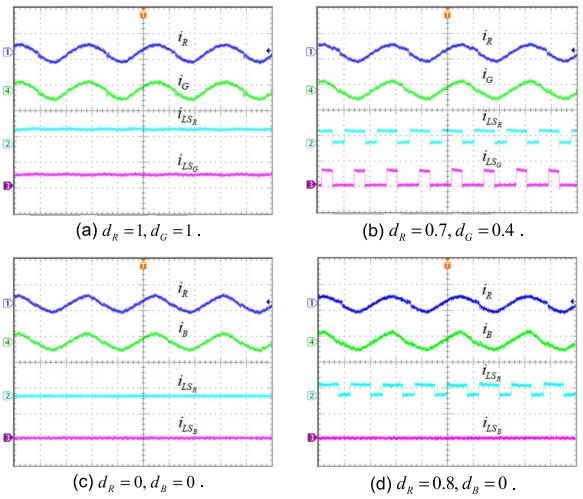

FIGURE 12. Current waveforms of the input module and LED strings (i_R, i_G, i_B: 2A/div, i_{LS_R}, i_{LS_G}, i_{LS_B}: 500mA/div, Timebase: 4μs /div).

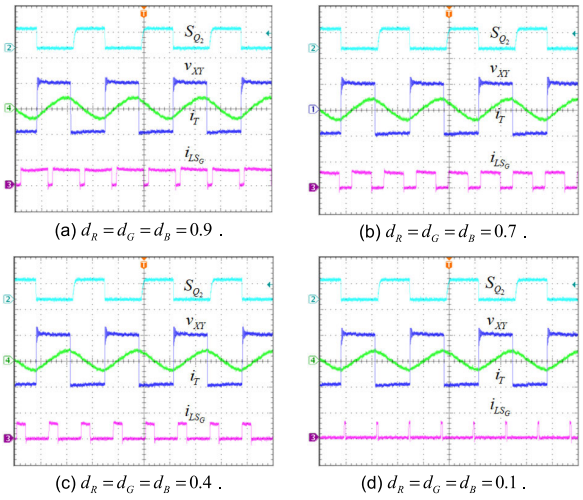

FIGURE 13. Key waveforms at different duty cycle of LED strings (i_{LS_G}: 500mA/div, v_{XY}: 50V/div, i_T: 5A/div, S_{Q_2}: 20V/div, Timebase: 4μs /div).

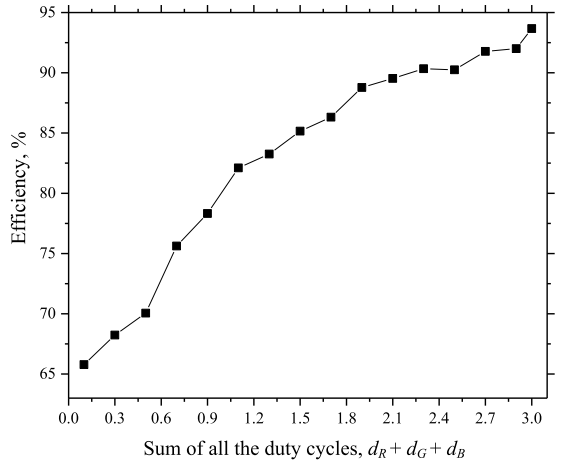

FIGURE 14. Efficiency versus the sum of all the duty cycles of RGB channels.

sum of all the duty cycles of RGB channels. It can be seen that the efficiency is higher than 80% when the sum of all the duty cycles of RGB channels is larger than 1 (the output power is about 12 W when $d_R + d_G + d_B = 1$) The maximum efficiency is around 93.67% when the sum of all the duty cycle is 3 (the output power is about 36W when $d_R + d_G + d_B = 3$). The minimum efficiency is around 65.78% when the sum of all the duty cycles is 0.1 (the output power is about 1.2W when $d_R + d_G + d_B = 0.1$).

IV. CONCLUSION

A fully decoupled current control and current balancing of the modular structure for LED color mixing system has been proposed. Compared with the conventional structure, the proposed topology has the merits of 1) no cross-coupling issues, 2) no current spike flowing through LEDs, 3) Current-balancing function for different color LED strings, 4) Non-isolated gate-driver circuits and 5) modularity, high stability and safety. The proposed structure has been evaluated with RGB LED strings. Experimental results show that the proposed structure has a good current-balancing performance at different duty ratio of LEDs, the switches for controlling LED strings are fully decoupled, and the main switches are always soft-switching at the different diming levels.

REFERENCES

[1] M. Amsteus, S. Al-Shaaban, E. Wallin, and S. Gjoqvist, "Colors in marketing: A study of color associations and context (in) dependence," *Int. J. Bus. Social Sci.*, vol. 6, no. 3, pp. 32–45, Mar. 2015.

[2] S.-K. Liaw, H.-H. Chou, C.-J. Wu, M.-J. Chien, and C. Teng, "500 Mb/s OOK visible light communications using RGB-based LEDs," in *Proc. Int. Symp. Next-Gener. Electron. (ISNE)*, Taipei, Taiwan, May 2015, pp. 1–2.

[3] R. Bell. (Feb. 2013). *Color Control of LED Lights*. [Online]. Available: https://www.musson.com/media/Downloads/Education/Pathway_ColorMixing.pdf

[4] X. Zhang, Y. Wang, Z. Lv, and D. Xu, "A LEDs light system based on color coordinates feedback for the projector," in *Proc. Int. Conf. Elect. Mach. Syst. (ICEMS)*, Dec. 2010, pp. 68–72.

[5] S. Muthu and J. Gaines, "Red, green and blue LED-based white light source: Implementation challenges and control design," in *Proc. 38th IAS Annu. Meeting Conf. Rec. Ind. Appl. Conf.*, 2003, pp. 515–522.

[6] S. J. Cheng, H. J. Chiu, C. J. Yao, and S. C. Mou, "Current and white-balance controls of an RGB LED backlight power supply system," in *Proc. SICE Annu. Conf.*, Aug. 2008, pp. 233–236.

[7] M. G. V. Bautista, W. R. Liou, and M. L. Yeh, "Dimmable multi-channel RGB LED driver," in *Proc. IEEE ECCE Asia Downunder*, Aug. 2013, pp. 1259–1262.

[8] Y. N. Chang, C. C. Hung, S. C. Tung, and S.-Y. Chan, "Auto mixed light for RGB LED backlight module," in *Proc. IEEE Int. Symp. Ind. Electron.*, Jul. 2009, pp. 864–869.

[9] H.-T. Chen, S.-C. Tan, and S. Y. Hui, "Nonlinear dimming and correlated color temperature control of bicolor white LED systems," *IEEE Trans. Power Electron.*, vol. 30, no. 12, pp. 6934–6947, Dec. 2015.

[10] K. Modepalli and L. Parsa, "A scalable N-color LED driver using single inductor multiple current output topology," *IEEE Trans. Power Electron.*, vol. 31, no. 5, pp. 3773–3783, May 2016.

[11] S. Zhou, G. Zhou, G. Liu, and G. Mao, "Small-signal modeling and cross-regulation suppressing for current-mode controlled single-inductor dual-output DC–DC converters," *IEEE Trans. Ind. Electron.*, vol. 68, no. 7, pp. 5744–5755, Jul. 2021.

[12] S. K. Ng, K. H. Loo, Y. M. Lai, and C. K. Tse, "Color control system for RGB LED with application to light sources suffering from prolonged aging," *IEEE Trans. Ind. Electron.*, vol. 61, no. 4, pp. 1788–1798, Apr. 2014.

[13] S. Dietrich, S. Strache, R. Wunderlich, and S. Heinen, "Get the LED out: Experimental validation of a capacitor-free single-inductor, multiple-output LED driver topology," *IEEE Ind. Electron. Mag.*, vol. 9, no. 2, pp. 24–35, Jun. 2015.

[14] C. P. G. Wong, A. T. L. Lee, K. Li, S.-C. Tan, and S. Y. Hui, "Precise luminous flux and color control of dimmable red-green-blue light-emitting diode systems," *IEEE Trans. Power Electron.*, vol. 37, no. 1, pp. 588–606, Jan. 2022.
[15] Y. Guo, S. Li, A. T. L. Lee, S.-C. Tan, C. K. Lee, and S. Y. R. Hui, "Single-stage AC/DC single-inductor multiple-output LED drivers," *IEEE Trans. Power Electron.*, vol. 31, no. 8, pp. 5837–5850, Aug. 2016.
[16] A. T. L. Lee, J. K. O. Sin, and P. C. H. Chan, "Scalability of quasi-hysteretic FSM-based digitally controlled single-inductor dual-string buck LED driver to multiple strings," *IEEE Trans. Power Electron.*, vol. 29, no. 1, pp. 501–513, Jan. 2014.
[17] H. Chen, Y. Zhang, and D. Ma, "A SIMO parallel-string driver IC for dimmable LED back lighting with local bus voltage optimization and single time-shared regulation loop," *IEEE Trans. Power Electron.*, vol. 27, no. 1, pp. 452–462, Jan. 2012.
[18] X. Zhan, H. Chung, and R. Zhang, "Investigation into the use of single inductor for driving multiple series-connected LED channels," *IEEE Trans. Power Electron.*, vol. 32, no. 4, pp. 3034–3050, Apr. 2017.
[19] C. S. Wong, K. H. Loo, H. H.-C. Iu, Y. M. Lai, M. H. L. Chow, and C. K. Tse, "Independent control of multicolor-multistring LED lighting systems with fully switched-capacitor-controlled LCC resonant network," *IEEE Trans. Power Electron.*, vol. 33, no. 5, pp. 4293–4305, May 2018.
[20] R. Zhang and H. S.-H. Chung, "Capacitor-isolated multistring LED driver with daisy-chained transformers," *IEEE Trans. Power Electron.*, vol. 30, no. 7, pp. 3860–3875, Jul. 2015.
[21] R. Zhang and H. S.-H. Chung, "Transformer-isolated resonant driver for parallel strings with robust balancing and stabilization of individual LED current," *IEEE Trans. Power Electron.*, vol. 29, no. 7, pp. 3694–3708, Jul. 2014.
[22] R. Zhang, X. Wu, H. S.-H. Chung, and X. Pan, "A color-theory-based chromaticity coordinates tracking strategy for LED color-mixing system," *IEEE Trans. Power Electron.*, vol. 36, no. 3, pp. 3269–3278, Mar. 2021.
[23] R. Zhang, H. S.-H. Chung, X. Wu, X. Wu, X. Zhang, and J. Wang, "Capacitor-isolated structure with brightness and color controlling for multicolor LED strings," in *Proc. IEEE Energy Convers. Congr. Expo. (ECCE)*, Oct. 2017, pp. 2023–2830.
[24] X. Zhan, W. Wang, and H. Chung, "A neural-network-based color control method for multi-color LED systems," *IEEE Trans. Power Electron.*, vol. 34, no. 8, pp. 7900–7913, Aug. 2019.
[25] X. Zhan, W. Wang, and H. S.-H. Chung, "A novel color control method for multicolor LED systems to achieve high color rendering indexes," *IEEE Trans. Power Electron.*, vol. 33, no. 10, pp. 8246–8258, Oct. 2018.

RUIHONG ZHANG (Member, IEEE) received the B.Eng. degree in computer science the M.Eng. degree in electrical engineering from the Harbin Institute of Technology, China, in 2005 and 2008, respectively, and the Ph.D. degree in electrical engineering from the City University of Hong Kong, Hong Kong, in 2013. She was a Postdoctoral Fellow with the City University of Hong Kong, from 2014 to 2015. She was an Associate Professor with Northwestern Polytechnical University, Xi'an, China, from 2016 to 2018. Since 2018, she has been with the Harbin Institute of Technology, Shenzhen, where she is an Associate Professor with the School of Mechanical Engineering and Automation. Her current research interests include lighting systems, wireless power transfer, power-factor-correction, resonant converters, ac/dc converters, dc/dc converters, and matrix converters.

ZHENG CAO was born in Hubei, China, in 1999. He received the B.S. degree in electrical engineering from the Harbin Institute of Technology, Harbin, China, in 2020. He is currently pursuing the M.S. degree in electrical engineering with the Harbin Institute of Technology, Shenzhen, China. His research interests include parallel operation of SiC MOSFETs and LED driver.

LINGLING CAO (Member, IEEE) received the B.S. and M.S. degrees in electrical engineering from the Nanjing University of Aeronautics and Astronautics, Nanjing, China, in 2008 and 2011, respectively, and the Ph.D. degree in electronic and information engineering from The Hong Kong Polytechnic University, Hong Kong, in 2015.

She is currently an Associate Professor with the Harbin Institute of Technology, Shenzhen. Her research interests include power converter topologies and control strategies for renewable energy systems.

E. PENG (Member, IEEE) received the B.E., M.E., and Ph.D. degrees from the Harbin Institute of Technology, Harbin, China, in 2002, 2004, and 2009, respectively.

He is currently a Professor with the Harbin Institute of Technology and the Head of the "Space Plasma Environment Simulation and Research System" of the national major science and technology infrastructure "Space Environment Simulation and Research Infrastructure." His current research interests include plasma flow control and its application and special power supply.